Characteristics of the single-longitudinal-mode planar-waveguide external cavity diode laser at 1064 nm

Kenji Numata,[1,2,*] Mazin Alalusi,[3] Lew Stolpner,[3] Georgios Margaritis,[3] Jordan Camp,[2] and Michael Krainak[2]

[1]*Department of Astronomy, University of Maryland, College Park, Maryland 20742, USA*

[2]*NASA Goddard Space Flight Center, Greenbelt, Maryland 20771, USA*

[3]*Redfern Integrated Optics Inc., 3350 Scott Blvd., No. 62, Santa Clara, California 95054, USA*

**Corresponding author: kenji.numata@nasa.gov*

Received January 15, 2014; revised February 26, 2014; accepted February 28, 2014; posted March 3, 2014 (Doc. ID 204793); published March 28, 2014

We describe the characteristics of the planar-waveguide external cavity diode laser (PW-ECL). To the best of our knowledge, it is the first butterfly-packaged 1064 nm semiconductor laser that is stable enough to be locked to an external frequency reference. We evaluated its performance from the viewpoint of precision experiments. Using a hyperfine absorption line of iodine, we suppressed its frequency noise by a factor of up to 10^4 at 10 mHz. The PW-ECL's compactness and low cost make it a candidate to replace traditional Nd:YAG nonplanar ring oscillators and fiber lasers in applications that require a single longitudinal mode.

OCIS codes: (140.2020) Diode lasers; (140.3425) Laser stabilization.
http://dx.doi.org/10.1364/OL.39.002101

Among the many types of lasers, single-longitudinal-mode lasers exhibit high coherence and can be used in such applications as interferometric sensing and high-resolution spectroscopy. We have shown that the planar-waveguide external cavity diode laser (PW-ECL), which was developed for 1550 nm telecom technologies, has a sufficiently low level of noise for precision measurement applications [1,2]. For example, the 1550 nm PW-ECL has been adopted for the Optical Testbed and Integration on ISS eXperiment (OpTIIX) project [3] and may eventually be deployed as an interferometric metrology laser source in space, where small mass, low cost, and high reliability are crucial. Researchers have also shown that 1550 nm PW-ECL can be frequency-stabilized to a high-finesse optical cavity and could serve as a replacement for fiber lasers in long optical links [4].

However, 1064 nm is the most commonly used wavelength in extreme sensing applications, including interferometric gravitational-wave detectors [5]. The standard for low-noise applications is the 1064 nm Nd:YAG nonplanar ring oscillator (NPRO) [6]. This wavelength is dominant because high-quality optics have been developed around the Nd:YAG laser, and a shorter wavelength offers higher phase sensitivity and smaller beam divergence. Although the Yb fiber laser has been investigated as a potential alternative, it does not present clear advantages over NPRO in cost, size, and noise. In this Letter, we describe the characteristics of the 1064 nm PW-ECL, which we are developing as a possible alternative to the larger, more complex NPRO. This work was originally motivated by the Laser Interferometer Space Antenna (LISA) mission [7] (now known as eLISA [8] in Europe) and the Gravity Recovery and Climate Experiment (GRACE)-II mission [9]. The commercial single-frequency distributed feedback (DFB) and distributed Bragg reflector (DBR) lasers at 1064 nm do not meet our applications' stringent low-noise and narrow-linewidth requirements. We believe that our PW-ECL is the lowest-noise semiconductor laser operating at 1064 nm in a butterfly package. Unlike bulk crystal or fiber lasers, the PW-ECL requires only one active laser media and costs approximately 10 times less. In order to investigate its suitability for precision experiments, we stabilized its frequency by locking to a hyperfine absorption line of iodine and by measuring its basic characteristics. The simplicity and performance of the PW-ECL make it an attractive alternative to traditional lasers at 1064 nm.

The 1064 nm PW-ECL tested was designed, developed, and built by Redfern Integrated Optics [10] and commercialized under the name PLANEX. Details of the technologies associated with the PW-ECL have been disclosed in [11]. Figure 1 (Left) shows a schematic of the PW-ECL. The laser cavity consists of two reflectors: (1) a high-reflective coated facet on a ridge-waveguide, GaAs-based gain chip and (2) an antireflection-coated waveguide grating formed in a silica-on-silicon planar lightwave circuit (PLC). All components are integrated on top of a thermoelectric cooler (TEC). The output is coupled to a polarization-maintaining fiber within a 14-pin butterfly package after the lens and the optical isolator.

The PW-ECL's high frequency stability results from its long effective cavity length as a semiconductor laser and from its detuned loading [12], which uses dispersive component (PLC gratings) as an external mirror. Because of the dispersive mirror, perturbations to frequency cause a change in the cavity loss rate, which

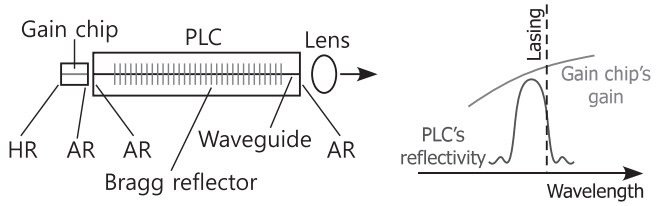

Fig. 1. (Left) Schematic of the PW-ECL. (See main text for definitions of abbreviations.) (Right) Relationship among the lasing wavelength, PLC gratings' reflectivity, and gain chip's gain.

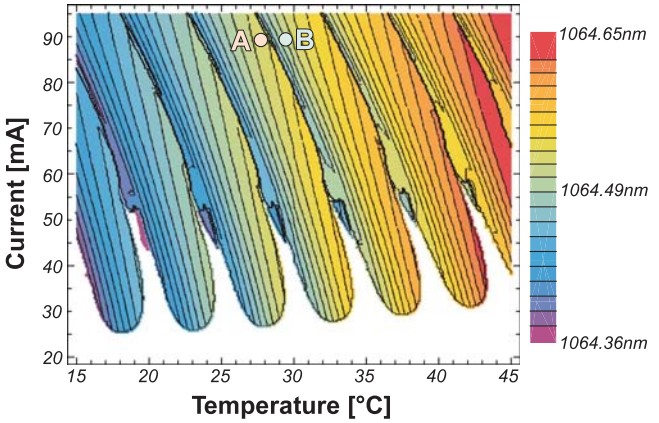

Fig. 2. Measured output wavelength dependence on the injection current and TEC temperature. A and B indicate the two (optimal and nonoptimal) operating points tested.

in turn changes operating point carrier density, and thus the cavity's refractive index. This produces a correction to the frequency at the longer wavelength side of the negative slope of the gratings' reflectivity curve [Fig. 1 (Right)] [13], stabilizing the frequency and ensuring single-mode operation.

Figure 2 shows the measured wavelength tuning of the PW-ECL by temperature and current adjustment. As the TEC temperature is raised, the gain chip's center wavelength and the PLC gratings' central reflectivity wavelength both increase. The gain chip's center wavelength also rises with the injection current due to carrier and temperature induced refractive index changes. Since the wavelength tuning characteristics of the gain chip and the PLC are different, the PW-ECL exhibits mode hops (the discontinuities in Fig. 2) with changing current and temperature. Within our measurement range, the PW-ECL is tuned from 1064.36 to 1064.65 nm (77 GHz range), which overlaps with the range of the typical Nd:YAG laser.

Figure 3 shows the measured output power dependence on the temperature and injection current. The change of the operating point within the PLC gratings' reflectivity curve directly affects the output power. The maximum output power at the optimum operating point is 15 mW. Near this point (marked A in Figs. 2 and 3), the lasing wavelength is off from the gratings'

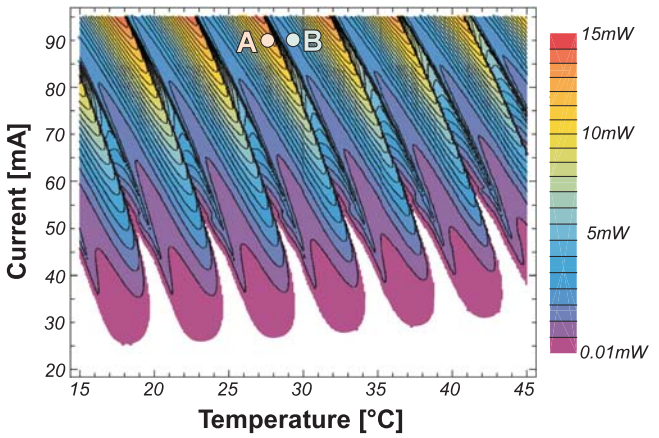

Fig. 3. Measured output power dependence on the injection current and TEC temperature.

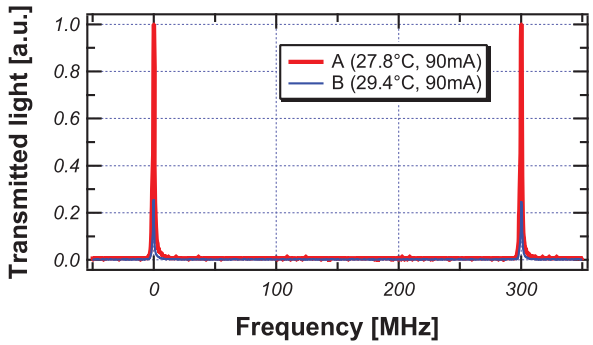

Fig. 4. Output optical spectra measured by a scanning FP.

reflectivity peak, and frequency noise is minimized (shown later). To the contrary, the regions with low output power (e.g., the point marked B) are closer to the peak and are not at the optimum, which offers the best noise performance.

As a result of comprehensive design, the PW-ECL emits a single-longitudinal-mode output at any stable operating point. Figure 4 shows the PW-ECL's transmitted light from a scanning Fabry–Perot (FP) interferometer with a 300 MHz free spectral range as detected at the two test operating points, A and B. Limited by the scanning FP's resolution of approximately 1 MHz, they gave evidence of a stable, single-mode lasing with no side modes.

The wavelength and power can be tuned quickly by modulating the injection current. Figures 5 and 6 show the frequency- and power-tuning responses as a function of the modulation frequency of the additive injection current. We used a low-noise current driver that has >10 MHz current modulation bandwidth [14] to measure the laser's response to the injection current directly (unlike we did for the 1542 m PW-ECL in [1]). The tuning amplitudes depend upon the location of the operating point in Figs. 2 and 3. In Figs. 5 and 6, the measured results at the two test operating points are plotted. At one optimal operating point (A), the frequency (wavelength) is relatively insensitive to the current variation. Therefore, it results in a smaller frequency-tuning amplitude compared to a nonoptimal operating point (B), as shown in Fig. 5. Power tuning produces smaller differences (Fig. 6). The 3 dB tuning bandwidth is approximately 40 and 100 kHz in the frequency and power tuning, respectively. The thermal nature of frequency tuning

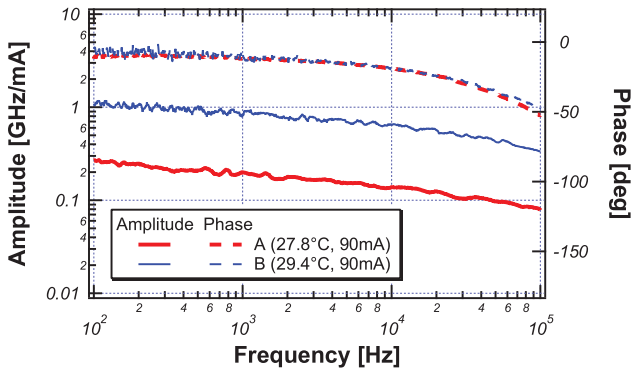

Fig. 5. Frequency-tuning transfer function.

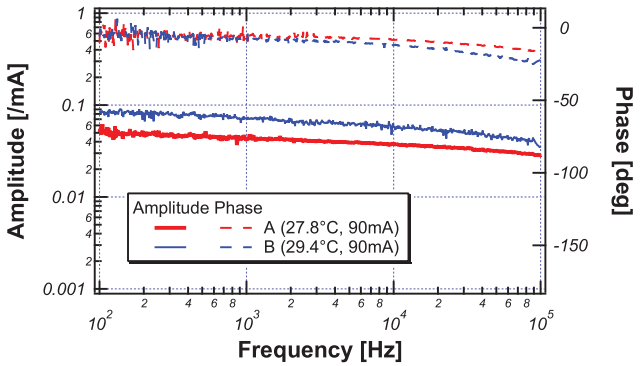

Fig. 6. Power-tuning transfer function.

caused its narrower bandwidth and larger phase delay. At a low frequency, 1 mA current modulation (on top of the 90 mA constant injection current) simultaneously introduces approximately 0.5 GHz frequency modulation and approximately 10% power modulation. This frequency-to-intensity coupling ($\sim 2 \times 10^{-4}$/MHz) is approximately 10 times larger than the piezo tuning in the NPRO [15].

Figure 7 shows the PW-ECL's free-running frequency noise at the two operating points as a function of Fourier frequency f. The frequency noise of the commercial Nd:YAG NPRO is also plotted for comparison. Since the lasing point is detuned, the optimal operating point (A) produces approximately five times less noise than the nonoptimal operating point (B) above a few Hz. Below 0.1 Hz, the PW-ECL makes frequency noise comparable to the NPRO. Above 10 Hz, the noise drops by $1/\sqrt{f}$ and $1/f$ for the PW-ECL and NPRO, respectively; therefore their difference becomes larger at a higher frequency. At 10 kHz, the PW-ECL produces approximately 100 times higher frequency noise than the NPRO.

We stabilized the PW-ECL's frequency using the optical heterodyne saturation spectroscopic technique [16] and an iodine cell. In an existing iodine stabilization system [17], we replaced an NPRO with the PW-ECL, followed by a dual-stage Yb-fiber amplifier. The amplifier's output was frequency doubled by a nonlinear crystal, and the generated 532 nm light used to probe the Doppler-free absorption line of iodine. The frequency error signal was fed back to the injection current. For this measurement, the PW-ECL was tuned to 1064.490 nm, whose

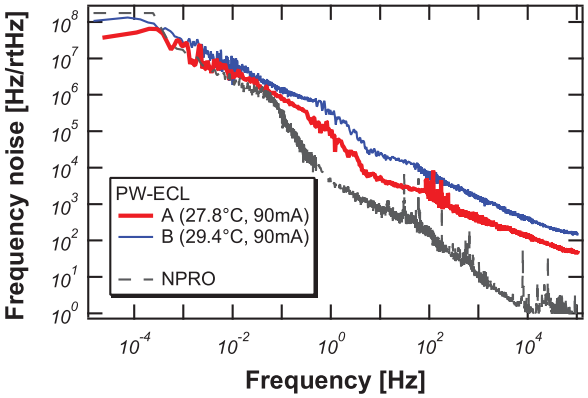

Fig. 7. Frequency noise of NPRO and PW-ECL at the two operating points.

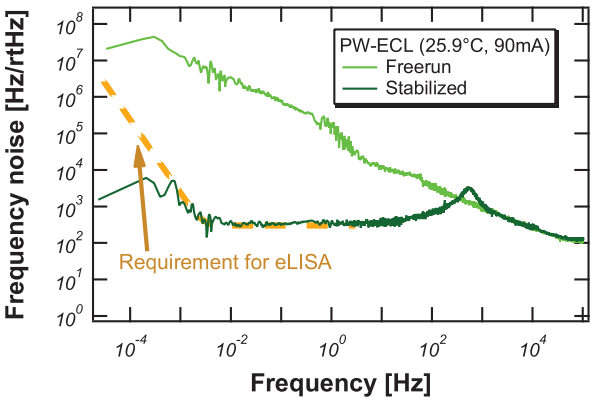

Fig. 8. Frequency noise of the PW-ECL with and without frequency stabilization.

doubled frequency coincides with the standard R(56)32-0 a_{10} line [18]. The lock was not lost over several days in a standard lab environment. Figure 8 shows the stabilized frequency noise spectrum, the free-running noise spectrum, and the eLISA's requirement at low Fourier frequency. Within the control bandwidth of approximately 300 Hz, the frequency noise was suppressed by a factor up to 10^4, reaching 300 Hz/$\sqrt{\text{Hz}}$. We believe that the noise floor is limited by the signal-to-noise ratio of the saturation signal, not by the PW-ECL itself.

Figure 9 compares the relative intensity noise (RIN) of the PW-ECL at the two operating points to the NPRO. The PW-ECL has smaller RIN than the NPRO below approximately 3 MHz. The difference between the two operating points is small. The NPRO has a relaxation oscillation peak around 700 kHz and reaches a shot noise level above approximately 6 MHz. The PW-ECL has a damped relaxation oscillation peak at a few GHz, much higher than the beat-note frequency of typical heterodyne measurement systems. The PW-ECL has a flat RIN level of $8 \times 10^{-9}/\sqrt{\text{Hz}}$ above approximately 2 MHz, which is approximately 1.2 times higher than the shot noise limit for the full optical power (~13 mW). The bump structure around 10 Hz is believed to be mostly from the air turbulence, which in part couples to the beam pointing, since the structure commonly appears in RIN measurements performed in the air, and it is dependent on the external measurement conditions.

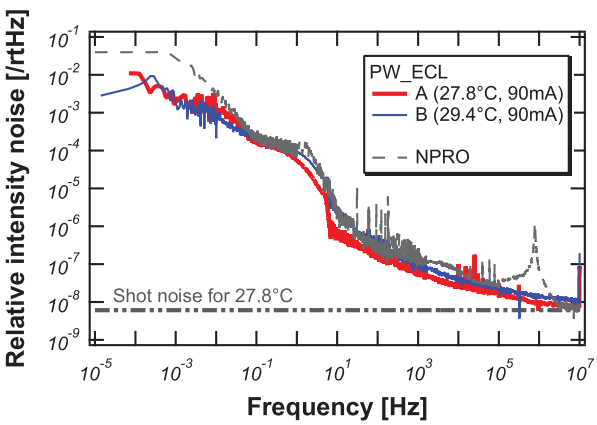

Fig. 9. RIN of NPRO and PW-ECL at the two operating points.

From the viewpoint of precision experiments, the major difference between the PW-ECL and the NPRO is the PW-ECL's higher frequency noise at a high Fourier frequency. Unless suitably pre-stabilized, continuously tracking its optical phase in high-precision heterodyne interferometry would be difficult due to the high-frequency jitter in the beatnote (the problem known as "cycle slip" in phase measurement systems [19]). For the same reason, external frequency actuators would be required to lock the PW-ECL directly to a cavity with very high finesse, in order to make the instantaneous linewidth narrower than the cavity's narrow bandwidth. We were able to lock the 1064 nm PW-ECL to a low-finesse (2000) cavity only by controlling the injection current. Therefore, the PW-ECL would be an excellent choice for use with a low-finesse cavity (e.g., injection seeding Nd:YAG lasers), replacing such bulky lasers as NPROs and fiber lasers.

In summary, we characterized the 1064 nm planar-waveguide external cavity laser, PW-ECL, which to our knowledge is the first semiconductor laser that emits a highly-stable, single-longitudinal-mode at 1064 nm in a butterfly package. We showed that the PW-ECL has the potential to replace traditional lasers at a lower cost and with a smaller footprint. With additional design iterations we can further improve its frequency noise performance in order to meet the requirements of the most demanding applications.

This research was funded by the NASA Small Business Innovation Research (SBIR) program.

References

1. K. Numata, J. Camp, M. A. Krainak, and L. Stolpner, Opt. Express **18**, 22781 (2010).
2. M. Alalusi, P. Brasil, S. Lee, P. Mols, L. Stolpner, A. Mehnert, and S. Li, Proc. SPIE **7316**, 73160X (2009).
3. M. Postman, W. B. Sparks, F. Liu, K. Ess, J. Green, K. G. Carpenter, H. Thronson, and R. Goullioud, Proc. SPIE **8442**, 84421T (2012).
4. C. Clivati, A. Mura, D. Calonico, F. Levi, G. A. Costanzo, C. E. Calosso, and A. Godone, IEEE Trans. Ultrason. Ferroelectr. Freq. Control **58**, 2582 (2011).
5. B. Barish and R. Weiss, Phys. Today **52**(10), 44 (1999).
6. T. J. Kane and R. L. Byer, Opt. Lett. **10**, 65 (1985).
7. K. Danzmann, and the LISA Study Team, Class. Quantum Grav. **13**, A247 (1996).
8. https://www.elisascience.org/.
9. W. M. Folkner, G. deVine, W. M. Klipstein, K. McKenzie, R. Spero, R. Thompson, N. Yu. M. Stephens, J. Leitch, R. Pierce, T. T.-Y. Lam, and D. A. Shaddock, in Proceedings of the 2011 Earth Science Technology Forum (2011).
10. Redfern Integrated Optics Inc., http://www.rio-inc.com (California, USA).
11. M. Alalusi, P. Mols, and L. Stolpner, "Achieving low phase noise in external cavity laser implemented using planar lightwave circuit technology," U.S. patent 8,295,320 B2 (October 23, 2012).
12. K. Vahala and A. Yariv, Appl. Phys. Lett. **45**, 501 (1984).
13. K. Vahala, "Dynamic and spectral features of semiconductor lasers," Ph.D. thesis (California Institute of Technology, 1985), Chapter 4.
14. C. J. Erickson, M. V. Zijll, G. Doermann, and D. S. Durfee, Rev. Sci. Instrum. **79**, 073107 (2008).
15. V. Quetschke, "Korrelationen von rauschquellen bei Nd:YAG lasersystemen," Ph.D. thesis (Universit at Hannover, 2003).
16. J. L. Hall, L. Hollberg, T. Baer, and H. G. Robinson, Appl. Phys. Lett. **39**, 680 (1981).
17. K. Numata and J. Camp, Appl. Opt. **47**, 6832 (2008).
18. J. Ye, L. Robertsson, S. Picard, L.-S. Ma, and J. L. Hall, IEEE Trans. Instrum. Meas. **48**, 544 (1999).
19. G. Ascheid and H. Meyr, IEEE Trans. Commun. **30**, 2228 (1982).